Available online at www.sciencedirect.com
ScienceDirect
Journal of Power Sources 158 (2006) 1096–1101
JOURNAL OF POWER SOURCES
www.elsevier.com/locate/jpowsour

Electrochemical behaviour of bismuth in sulfuric acid solution

W.S. Li [a,*], X.M. Long [a], J.H. Yan [a,b], J.M. Nan [a], H.Y. Chen [a], Y.M. Wu [a]

[a] *Department of Chemistry, South China Normal University, Guangzhou 510631, China*
[b] *B.B. Battery Co., Ltd., Raoping, Guangdong 515700, China*

Received 21 September 2005; accepted 30 January 2006
Available online 4 April 2006

Abstract

Bismuth is considered to be a detrimental element to lead–acid batteries because it has lower hydrogen evolution overpotential than lead. On the other hand, bismuth can improve the performances of negative or positive active-materials. It is necessary to understand the performance of bismuth in sulfuric acid solution in order to reduce its detrimental effect on lead–acid batteries and make good use of its beneficial aspects. In this paper, the electrochemical behaviour of bismuth in sulfuric acid solution is studied by cyclic voltammetry (CV), chronoamperometry (CA), electrochemical impedance spectroscopy (EIS), scanning electronic spectroscopy (SEM), and X-ray diffraction (XRD). At potentials near close to the open-circuit value bismuth dissolves actively when it is anodized. As the potential increases, two oxidation peaks are observed. The first peak corresponds to the formation of bismuth sulfate, that follows a dissolution–precipitation mechanism and suppresses the dissolution of bismuth. The second peak due to secondary oxidation of bismuth under the bismuth sulfate film. There is a large current plateau at higher potentials this involves the dissolution of bismuth sulfate into solution, the formation of bismuth sulfate from bismuth oxide, and the formation of bismuth oxide from matrix bismuth. Hydrogen evolution takes place on bismuth just after the potential where the reduction of lead sulfate is completed. Oxygen evolution cannot occur on bismuth covered with bismuth sulfate.

Keywords: Bismuth; Dissolution; Surface film; Lead–acid battery; Hydrogen and oxygen evolution; Overpotential

1. Introduction

Much interest has focused on the effect of bismuth on the performances of lead–acid batteries because this element is found to occur in lead ores and is difficult to separate from lead. The effect of bismuth on hydrogen evolution on lead is well understood [1–3]. There is less influence when bismuth is used in lead alloys, but bismuth accelerates hydrogen evolution when it is deposited on the lead surface from solution by a displacement reaction with lead. The effect of bismuth on oxygen evolution on lead alloys can also be neglected when its content in lead alloys is less than 0.1 wt.% [4]. Bismuth was thought to be one of the elements that can improve the performances of lead–acid batteries [5–8]. By contrast, controversial results have been obtained for the effect of bismuth on lead corrosion. Some researchers have disclosed that bismuth in lead alloys accelerates the lead corrosion [9–11], but others consider that bismuth in lead alloys inhibit the lead corrosion [12,13]. It is obvious that bismuth may play opposite roles in lead–acid batteries under different conditions. On the one hand, it can improve the battery performance, on the other hand it may produce a detrimental effect when it is used unsuitably.

It is necessary to understand the performance of bismuth in sulfuric acid solution in order to reduce any detrimental effect on lead–acid battery performance and to make good use of its possible beneficial aspects. In this study, the electrochemical behaviour of bismuth in sulfuric acid solution is examined by cyclic voltammetry, chronoamperometry, electrochemical impedance spectroscopy, X-ray diffraction, and scanning electronic spectroscopy.

2. Experimental

Electrochemical experiments were performed with PGSTAT-30 equipment (Autolab, Eco Echemie B. V Company) and a three-electrode cell. The bismuth electrode was used as the working electrode and was prepared as follows. Bismuth (99.999 wt.%) was melted, cast as a cylinder and sealed with

* Corresponding author. Tel.: +86 20 85211368; fax: +86 20 85216890.
E-mail address: liwsh@scnu.edu.cn (W.S. Li).

0378-7753/$ – see front matter © 2006 Elsevier B.V. All rights reserved.
doi:10.1016/j.jpowsour.2006.01.093

epoxy resin to leave a disk with a working surface that had diameter of 6.18 mm. A platinum electrode with a large area was used as the auxiliary electrode. The reference electrode was Hg/Hg_2SO_4/4.79 M H_2SO_4. All potential values are reported with respect to this reference electrode. Before each experiment, the working electrode was polished with silicon carbide paper of 1200 grit, washed with deionized and double-distilled water, and degreased with ethanol. The working surface was perpendicular to the solution surface during experiments to prevent the adherence of gas bubbles on the electrode. For measurements of electrochemical impedance (EIS), frequencies from 10^5 to 0.5 Hz were employed and the amplitude of the a.c. voltage was 10 mV.

X-ray diffraction (XRD) experiments were performed with a D/MAX-3A/Rigaku diffractor with Cu Kα radiation of 30 kV, 30 MA at 12° per min. Scanning electron microscopic (SEM) studies were performed with a HITACHI S-50 instrument.

3. Results and discussion

3.1. Electrochemical oxidation and reduction behaviour of bismuth electrode

A typical cyclic voltammogram for a bismuth electrode in 4.79 M H_2SO_4 solution is shown in Fig. 1. The open-circuit potential of bismuth is about −0.45 V, i.e., about 0.55 V more positive than that of lead. As the potential increases, the current increases rapidly at the beginning, then two anodic current peaks 'a' and 'b' appear at potentials of −0.2 and 0.3 V, respectively. Finally, the current remains almost unchanged. On reversal of the potential, one anodic current peak appears at 0 V and two cathodic current peaks 'c' and 'd' appears at about −0.5 and −0.8 V, respectively.

The current sustained by a bismuth electrode at different potentials is given in Fig. 2. At a potential of −0.4 V, which is near the open-circuit value, the current is very small. At the potential of −0.35 V, which is lower than the potential of peak 'a', the current becomes larger. At the potential of peak 'b' and the higher potentials, the currents are very large and less dependent of potential. These results are in good agreement with the voltammetric behaviour.

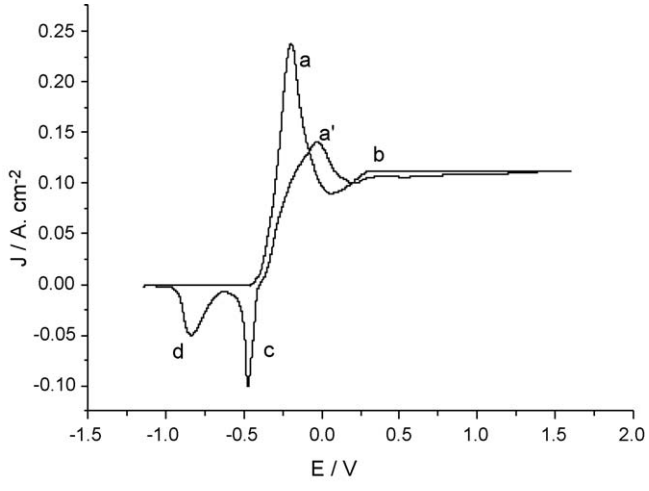

Fig. 1. Cyclic voltammogram for bismuth in 4.79 M H_2SO_4 scan rate: 20 mV s^{-1}.

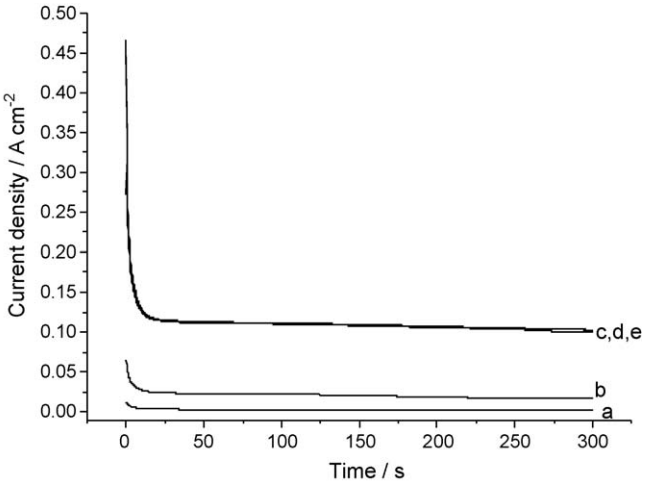

Fig. 2. Current correspondence of bismuth electrode in 4.79 M H_2SO_4 at different potentials: (a) −0.4 V, (b) −0.35 V, (c) 0.3 V, (d) 1.3 V and (e) 1.6 V.

To establish the mechanism for the anodic oxidation and the cathodic reduction of bismuth electrodes in sulfuric acid solution, other techniques are used such as SEM, XRD and EIS.

The scanning electron micrograph shown in Fig. 3(a) reveals the surface morphology of the bismuth electrode as-prepared. When the electrode is anodized at a potential close to the open-circuit potential, clear crystal grains and their interfaces can be seen, as shown in Fig. 3(b). This indicates that the electrode experiences an active dissolution process. Near the potential of peak 'a', a new phase is formed on the electrode surface, as seen in Fig. 3(c). This means that a deposition process takes place in concert with an active dissolution process as the current increases. At the potential where the current becomes constant, the deposited phase becomes smooth, as shown in Fig. 3(d).

X-ray diffraction patterns for bismuth electrodes before and after anodic oxidation at different potentials are given in Fig. 4. The curve 'a' is the XRD pattern for a bismuth electrode as-prepared. It is characteristic of bismuth crystals. When the electrode is anodized at a potential close to the open-circuit value, the characteristic diffraction peaks of bismuth crystals become sharper than those of curve 'a', as shown by curve 'b'. This is in agreement with the results obtained by SEM investigation. At a potential near the potential of peak 'a' of Fig. 1, the characteristic diffraction pattern for bismuth crystals disappears and the diffraction is very weak, see curve 'c'. The diffraction pattern virtually disappears when the current becomes constant, see curve 'd'. This indicates that the deposited phase is amorphous a feature that becomes more prominent as the potential increases.

The electrochemical impedance spectra obtained at different potentials are presented in Fig. 5. At −0.45 V, the Nyquist spectrum consists of a semicircle, which reflects a charge-transfer step at higher frequencies, and a straight line, which indicates a semi-infinite diffusion step at lower frequencies, as shown in Fig. 5(a). This behaviour demonstrates that the electrode reaction is mix-controlled by a charge-transfer step and diffusion step in the solution. At higher potentials, the semicircle still exists

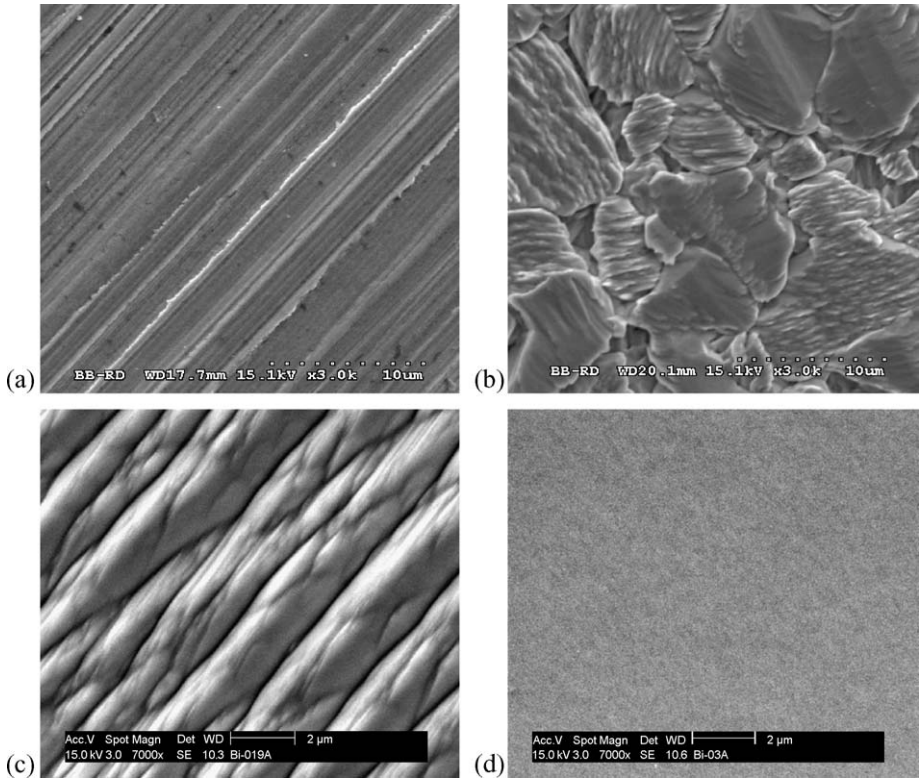

Fig. 3. Scanning electron micrographs of bismuth electrode before (a) and after anodic oxidation in 4.79 M H_2SO_4 at (b) −0.4 V (c), −0.2 V and (d) 0.3 V.

at higher frequencies and the straight line at lower frequencies becomes an arc, as shown in Fig. 5(b). The charge-transfer resistance (radius of the semicircle at higher frequencies) decreases with increasing potential. The arc at lower frequencies represents a diffusion step that involves a finite layer. This indicates that the deposited layer is formed at and very negative potentials, such as −0.35 V, and the diffusion step in the deposited layer becomes one of the two limiting steps of the electrode reaction. At a potential near peak 'a', a negative reaction resistance appears, as shown in Fig. 5(c), which is characteristic of a decrease in current with increasing potential [14,15]. This indicates that the electrode surface is covered completely by a deposited layer, that inhibits the anodic oxidation of bismuth. At potentials where the current becomes constant, the electrochemical impedance spectrum has more than two time constants, as shown in Fig. 5(d). This suggests that the electrode reaction process is complicated and involves more that two steps in this potential range.

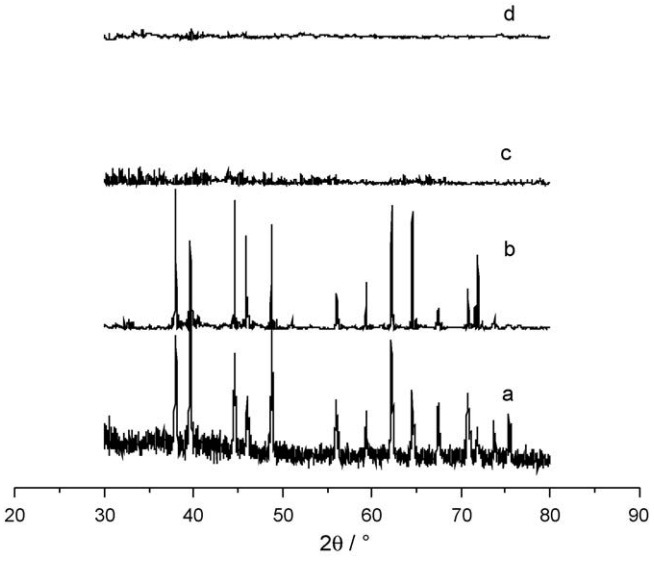

Fig. 4. X-ray diffraction pattern for bismuth electrode before (a) and after anodic oxidation in 4.79 M H_2SO_4 at −0.4 V (b), −0.2 V (c) and 0.3 V (d).

To identify the cause of the reduction peak 'c' in Fig. 1, linear voltammetry of bismuth electrode was carried out in a solution that contained dissolved bismuth ions. The result is shown in Fig. 6. It can be seen that the reduction peak potential of dissolved bismuth ions saturated in the solution is about −0.45 V, i.e., very close to the potential of peak 'c' in Fig. 1. Therefore, peak 'c' is corresponds to the reduction of bismuth ions.

To identify the reduction peak 'd' of Fig. 1, cyclic voltammetry was performed on a bismuth electrode in several sweep potential ranges with different upper reversal potentials. The results are shown in Fig. 7. When the upper reversal potential is higher than the potential of peak 'a' but lower than the potential of peak 'b' of Fig. 1, only peak 'c' but not peak 'd' can be observed, as shown in Fig. 7(a). The peak 'd' begins to appear when the upper reversal potential is higher than the potential of peak 'b', as shown in Fig. 7(b). The current of peak 'd' increases as the upper reversal potential increases, as shown in Fig. 7(c) and (d). This suggests that the reduction peak 'd' is not related to the deposition formed near the potential of peak 'a' but corresponds to compounds formed after the potential of peak 'b'.

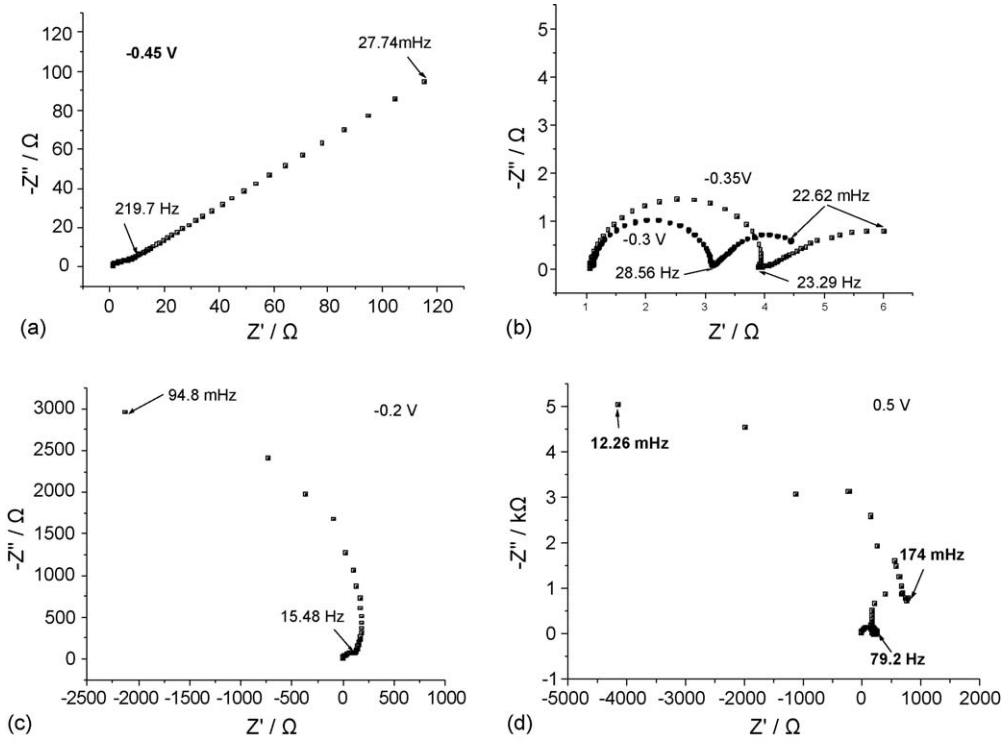

Fig. 5. Electro chemical impedance spectra of bismuth electrode in 4.79 M H_2SO_4 at given potentials.

X-ray diffraction data obtained for a bismuth electrode after being held at 1.3 V for 10 min and then at a given potential for 8 min are presented in Fig. 8. There is almost no diffraction, as shown in curve 'a' of Fig. 8. This indicates that the electrode surface is covered with an amorphous substance. This is easily understood because there is no diffraction for a bismuth electrode after anodic polarization at 0.3 V, as shown in the curve 'd' of Fig. 4. There is still no diffraction for the electrode after polarization at 1.3 V for 10 min and then at −0.45 V for 8 min, as shown in the curve 'b' of Fig. 8. Thus, the electrode surface is still covered with the amorphous substance, even though −0.45 V is very close to the open circuit potential.

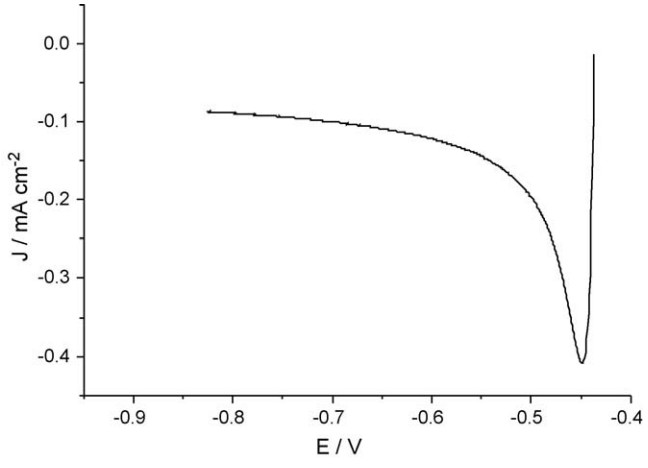

Fig. 6. Linear voltammogram of bismuth electrode in 4.79 M H_2SO_4 saturated with bismuth sulfate; scan rate: 20 mV s^{-1}.

3.2. Mechanism of electrochemical oxidation and reduction of bismuth

It is well known that there are many forms of dissolved bismuth ions in sulfuric acid solution and that bismuth oxide sulfate is amorphous. The simplest form of dissolved bismuth is BiO^+ and the simplest of bismuth oxide sulfates is $(BiO)_2SO_4$. Based on the results available, a mechanism can be deduced for the electrochemical oxidation and reduction of bismuth in sulfuric acid solution.

At anodic potentials close to the open-circuit value, bismuth experiences an active dissolution process, followed by the formation of dissolved bismuth ions, i.e.,

$$Bi + H_2O \rightarrow BiO^+ + 2H^+ + 3e^- \quad (1)$$

This reaction is mix-controlled by the charge-transfer step and the diffusion of BiO^+ into the bulk solution. When BiO^+ is accumulated on the electrode surface to a saturation concentration, the deposition process takes place:

$$2BiO^+ + {SO_4}^{2-} \rightarrow (BiO)_2SO_4 \quad (2)$$

Reaction (1) is inhibited when a monolayer of $(BiO)_2SO_4$ is formed on the surface of bismuth, and this results in a decrease of anodic oxidation current and the appearance of peak 'a' of Fig. 1. Reaction (2) is reversed when the surface concentration of BiO^+ is lower than its saturation concentration due to diffusion into the bulk solution. As the potential increases, the secondary oxidation of bismuth takes place under the monolayer of $(BiO)_2SO_4$ and causes the appearance of peak 'b', i.e.,

$$Bi + 2H_2O \rightarrow BiOOH + 3H^+ + 3e^- \quad (3)$$

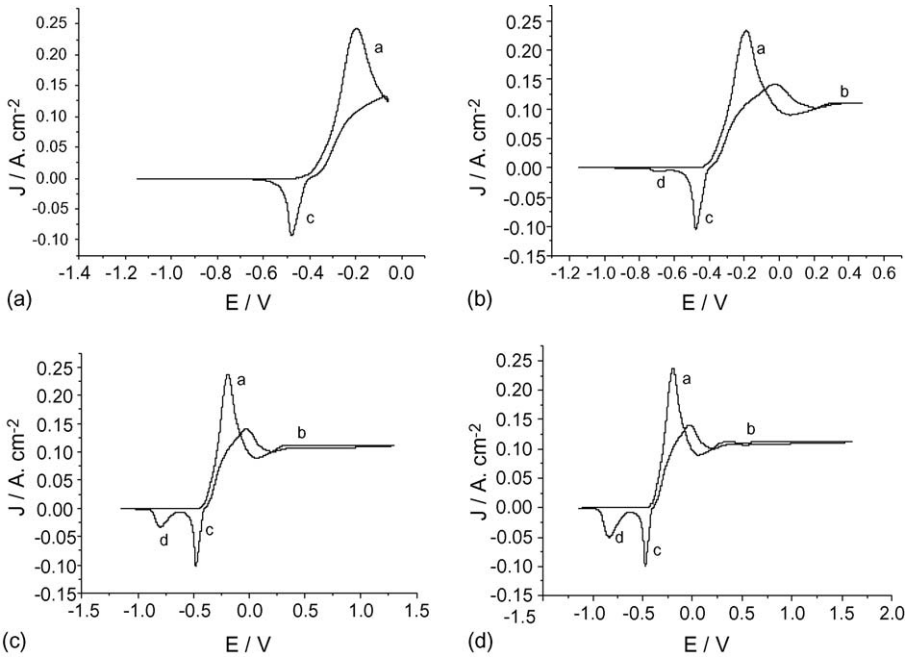

Fig. 7. Cyclic voltammogram of bismuth electrode in 4.79 M H_2SO_4 at different upper reversal potentials: (a) −0.06 V (b) 0.48 V (c) 1.3 V and (d) 1.6 V, scan rate: 20 mV s^{-1}.

Reaction (3) takes place because the monolayer of $(BiO)_2SO_4$ film is penetrable to H_2O and protons but not to sulfate ions, thus the BiOOH layer grows thicker and thicker as the potential increases further. The appearance of the constant current in Fig. 1 is due to a potential drop across the surface film on the electrode. A new layer of $(BiO)_2SO_4$ can be formed from the BiOOH if the old layer of $(BiO)_2SO_4$ dissolves due to the reversal reaction of (2), i.e.,

$$2BiOOH + 2H^+ + SO_4{}^{2-} \rightarrow (BiO)_2SO_4 + 2H_2O \quad (4)$$

When the potential is reversed to the open-circuit value, some of the electrode surface is exposed due to reaction (4) and the reversal of reaction (2). This is accompanied by reaction (1) and then the reversal reaction of (1) on the bare bismuth, resulting in the anodic current peaks 'a′' and cathodic current peak 'c' in Fig. 1, respectively. At a very negative potential, the residual $(BiO)_2SO_4$ formed via reaction (4) is reduced, resulting in peak 'd' of Fig. 1.

3.3. Hydrogen and oxygen evolution on bismuth electrode

A cyclic voltammogram of a bismuth electrode over a wide potential range is given in Fig. 9. A cyclic voltammogram of a lead electrode under the same conditions is shown in Fig. 10 for comparison. It can be seen from Fig. 9 that hydrogen evolution reaction takes place on bismuth electrode at about −1.23 V, as

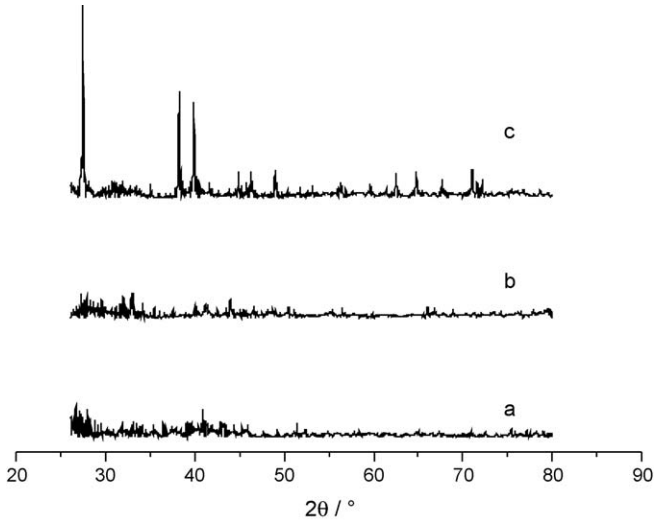

Fig. 8. X-ray diffraction patterns of bismuth electrode after anodic oxidation at 1.3 V and then cathodic reduction in 4.79 M H_2SO_4 at (a) 0.3 V, (b) −0.45 V and (c) −0.75 V.

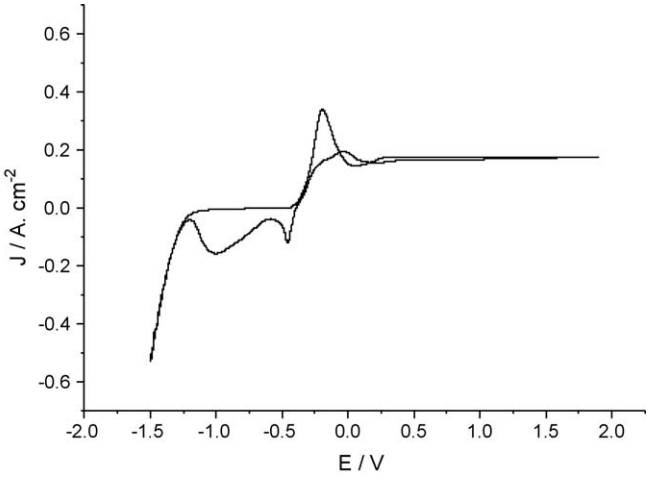

Fig. 9. Cyclic voltammogram of bismuth electrode in 4.79 M H_2SO_4 in a wide potential range, scan rate: 20 mV/s.

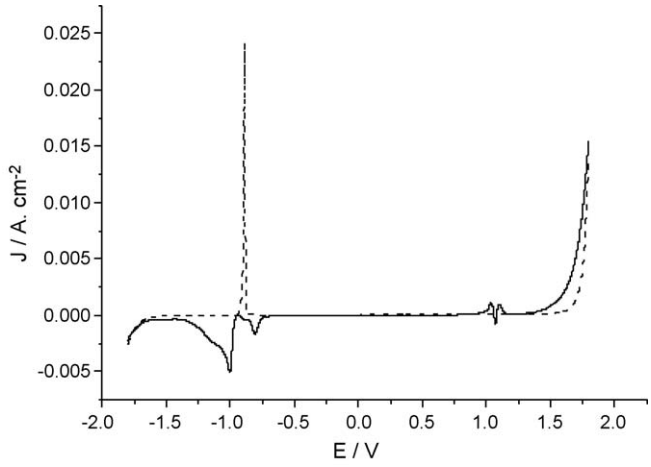

Fig. 10. Cyclic voltammogram of lead electrode in 4.79 M H_2SO_4 in a wide potential range, scan rate: 20 mV/s.

soon as reduction of the surface film on the electrode is completed. By contrast, hydrogen involves on a lead electrode at about −1.62 V, as shown in Fig. 10. It is obvious that bismuth has lower hydrogen evolution overpotential than lead, i.e., hydrogen evolution reaction takes place on bismuth more easily than on lead. It appears, therefore, the adverse effect of bismuth on lead–acid battery performance is not due to a low hydrogen evolution potential of bismuth because the reduction of lead sulfate as the discharge product of the negative electrode in lead–acid battery is almost completed at the potential for hydrogen evolution on bismuth, as shown in Fig. 10. It can also be seen from Fig. 9 that oxygen evolution reaction does not takes place on a bismuth electrode that is covered with a surface film even when the potential reaches 2 V. This is very different to oxygen evolution on lead that takes place on an electrode covered with lead sulfate.

4. Conclusion

The electrochemical behaviour of bismuth in sulfuric solution is very different from that of lead. The latter is easily passivated by lead sulfate when it is anodized. By contrast, bismuth experiences an active dissolution at a potential near to its open-circuit potential and sustains a large anodic current even when it is taken to a very positive potential. This behaviour results from the higher solubility of bismuth sulfate than lead sulfate. For bismuth, there are two anodic oxidation peaks on the positive-going potential sweep and two cathodic reduction peaks on the reverse sweep. The first oxidation peak results from the deposition of a monolayer of bismuth sulfate, which inhibits the anodic oxidation of bismuth. The second peak is due to the secondary oxidation of bismuth under the deposited bismuth sulfate. The first cathodic peak results from the reduction of bismuth ions dissolved in solution and the second from reduction of bismuth sulfate remaining on the electrode surface. Hydrogen evolution takes place on bismuth at a potential where the reduction of bismuth sulfate and lead sulfate is completed. Oxygen evolution cannot take place on a bismuth electrode covered with deposited bismuth sulfate.

Acknowledgements

This work was financially supported by national 863 project of China (2003AA302410), NSFC(20173018), EYTP of MOE, Key project of Guangdong Province (2003A1100401, 20042B08), GDSF(031533).

References

[1] M. Johnson, S.R. Ellis, N.A. Hampson, F. willamson, M.C. Ball, et al., J. Power Sources 22 (1988) 11.
[2] N. Papageorgjou, M. Skyllas-Kazacos, Electrochim. Acta 37 (1992) 269.
[3] Y.M. Wu, W.S. Li, X.M. Long, F.H. Wu, H.Y. Chen, J.H. Yan, C.R. Zhang, J. Power Sources 144 (2005) 338.
[4] W.S. Li, H.Y. Chen, X.M. Long, et al., J. Power Sources 158 (2006) 902.
[5] L.T. Lam, N.P. Haigh, O.V. Lim, D.A.J. Rand, J.E. Manders, J. Power Sources 78 (1999) 139.
[6] L.T. Lam, N.P. Haigh, D.A.J. Rand, J. Power Sources 88 (2000) 11.
[7] J.E. Manders, L.T. Lam, R. De Marco, J.D. Douglas, R. Pillig, D.A.J. Rand, J. Power Sources 48 (1994) 113.
[8] L.T. Lam, N.P. Haigh, D.A.J. Rand, J.E. Manders, J. Power Sources 88 (2000) 2.
[9] L.T. Lam, J.D. Douglas, R. Pillig, D.A.J. Rand, J. Power Sources 48 (1994) 219.
[10] M.W. Stevenson, C.S. Lakshmi, J.E. Manders, L.T. Lam, J. Power Sources 95 (2001) 264.
[11] S.J. Xia, W.F. Zhou, Electrochim. Acta 40 (1995) 181.
[12] N.A. Hampson, S. Kelly, K. Peters, J. Electrochem. Soc. 127 (1980) 1456.
[13] M.J. Koop, D.F.A. Koch, D.A.J. Rand, J. Power Sources 34 (1991) 69.
[14] W.S. Li, S.Q. Cai, J.L. Luo, J. Electrochem. Soc. 151 (2004) B220.
[15] W.S. Li, N. Cui, J.L. Luo, Electrochim. Acta 49 (2004) 1663.